

A Search for Environmental Effects on Type Ia Supernovae

Mario Hamuy

Steward Observatory, The University of Arizona, Tucson, AZ 85721

S. C. Trager¹

The Observatories of the Carnegie Institution of Washington, 813 Santa Barbara St., Pasadena, CA 91106

Philip A. Pinto

Steward Observatory, The University of Arizona, Tucson, AZ 85721

M. M. Phillips

Carnegie Institution of Washington, Las Campanas Observatory, Casilla 601, La Serena, Chile

R. A. Schommer

National Optical Astronomy Observatories², Cerro Tololo Inter-American Observatory, Casilla 603, La Serena, Chile

Valentin Ivanov

Steward Observatory, The University of Arizona, Tucson, AZ 85721

Nicholas B. Suntzeff

National Optical Astronomy Observatories², Cerro Tololo Inter-American Observatory, Casilla 603, La Serena, Chile

ABSTRACT

We use integrated colors and B and V absolute magnitudes of Type Ia supernova (SN) host galaxies in order to search for environmental effects on the SN optical properties. With the new sample of 44 SNe we confirm the conclusion by Hamuy et al. (1996a) that bright events occur preferentially in young stellar environments. We find also that the brightest SNe occur in the least luminous galaxies, a possible indication that metal-poorer neighbourhoods produce the more luminous events. The interpretation of these results is made difficult, however, due to the fact that galaxies with younger stellar

¹Hubble Fellow

²Cerro Tololo Inter-American Observatory, Kitt Peak National Observatory, National Optical Astronomy Observatories, operated by the Association of Universities for Research in Astronomy, Inc., (AURA), under cooperative agreement with the National Science Foundation.

populations are also lower in luminosity. In an attempt to remove this ambiguity we use models for the line strengths in the absorption spectrum of five early-type galaxies, in order to estimate metallicities and ages of the SN host galaxies. With the addition of abundance estimates from nebular analysis of the emission spectra of three spiral galaxies, we find possible further evidence that luminous SNe are produced in metal-poor neighborhoods. Further spectroscopic observations of the SN host galaxies will be necessary to test these results and assist in disentangling the age/metallicity effects on Type Ia SNe.

Subject headings: cosmology: distance scale — galaxies — supernovae

1. Introduction

The study of the Hubble diagram of nearby ($z \leq 0.1$) Type Ia supernovae (SNe, hereafter) has shown that these objects can be used as precise distance indicators through the application of the peak luminosity-light curve width relation (Phillips 1993, Hamuy et al. 1996b, Riess et al. 1996, Perlmutter et al. 1999). This method has been recently applied to distant ($0.3 \leq z \leq 1$) SNe to measure the values of the cosmological parameters. These studies have revealed a surprising cosmological result, namely, that the expansion of the Universe is presently accelerating due to a non-zero cosmological constant (Riess et al. 1998, Perlmutter et al. 1999). Even though this conclusion is based on several dozen of high- z events that permit the lowering of the statistical errors to significant levels, the reality of this result is threatened by the systematic errors that may result from comparison of distant events with those of the local Universe. Particularly relevant is the evolution of the stellar populations that produce the high- z SNe (with look-back times of 5-7 Gyr) which has the potential to affect the properties of the explosion and bias the determination of distances. It proves important therefore to investigate these effects from theoretical and observational point of views.

The effects of ages and metallicities of the SN progenitors in the properties of the SNe have been examined from a theoretical point of view using delayed detonation (DD) models of a Chandrasekhar-mass white dwarf (WD) by Höflich et al. (1998), who concluded that 1) old stellar populations contain WDs with C/O=1/1 that produce SNe with somewhat fainter peak luminosities (~ 0.1 mag) relative to SNe in younger environments containing WDs with C/O=2/3, and 2) a drop of 0.5 dex in the metallicity of the SN progenitor leaves the light curve shapes virtually unchanged and causes a slight decrease (0.03 mag) in the monochromatic B and V luminosities. Using DD models and the “strong wind” model for the mass-accretion phase of the WD, Umeda et al. (1999) reached the same conclusion, namely, that lower metallicity or older progenitors lead to dimmer SNe Ia, although the metallicity effects are more pronounced in these models due to opacity effects in the mass-accretion rate.

Since the local Universe produces SNe that explode in different stellar environments, the sample of nearby SNe offers the possibility to test these theoretical pre-

dictions and examine the origin of the diversity among SNe Ia. A first attempt using this approach based on the morphological classification of the host galaxies was performed by Hamuy et al. (1995, 1996a), who noticed that the most luminous SNe Ia were hosted by spiral (blue) galaxies. Using the Hamuy et al. (1995) sample of 13 distant SNe Ia and 10 nearby SNe, Branch et al. (1996) reached a similar conclusion, namely, that SNe in redder galaxies have lower luminosities. The goal of this paper is to go a step further and use all the information available to us on the SN host galaxies, in order to collect observational clues that could help us unveil the nature of SNe Ia and the relevant parameters that govern their optical properties. Ideally, a study of the effects of the stellar environments on the SN Ia explosions would require observations of the immediate stellar population that produced the SN but, in practice, this is difficult to perform. A more feasible observation, on the other hand, is that of the integrated light of the galaxy through an aperture containing a significant fraction of the total luminosity of the galaxy. Although this observation proves much easier to perform, the global properties of the stellar system might differ significantly from those of the site where the SN progenitor formed. An additional difficulty of this approach that hampers the interpretation of the results comes about from the observations of present-day stellar populations which might be significantly different than those where the SN progenitor was born. Given that the direct observation of a SN progenitor is unlikely, we proceed here with this indirect route, keeping in mind its limitations and the potential danger of extrapolating the nature of the host galaxy globally to the specific nature of the SN environment.

In this paper we focus both on photometric and spectroscopic data of the 62 galaxies that have hosted the best observed SNe. Section 2 describes the object sample and the photometric data that we employ to characterize the SN neighborhoods. In Section 3 we use this information and additional limited spectroscopic data available in the literature to study the relation of the SNe to the ages and metallicities of the host galaxies. In Section 4 we compare the observational results to the theoretical predictions, and we analyze the systematic effects of the environmental conditions in the determination of extragalactic distances. Finally, in Section 5 we summarize our conclusions.

2. Supernova Sample and Observations

In this paper we consider the 62 best-observed SNe Ia with $z < 0.1$ comprising the full sample of 29 Calán/Tololo SNe (Hamuy et al. 1996c), 20 objects from the “CfA” sample (Riess et al. 1999), and 13 nearby SNe Ia (SNe 1937C, 1972E, 1980N, 1981B, 1986G, 1989B, 1990N, 1991T, 1992A, 1994D, 1996X, and 1996bu). This is the same sample studied by Phillips et al. (1999) having precise BVI peak magnitudes, decline rates [$\Delta m_{15}(B)$], and color excesses, due to absorption in the host galaxy. Table 1 gives the full list of SNe, their decline rates, the name and Hubble type of the host galaxy. The morphological classifications come from 1) our own typing of the Calán/Tololo SN host galaxies¹, 2) the NASA/IPAC Extragalactic Database² (<http://nedwww.ipac.caltech.edu/>), and 3) Riess et al. (1999), in this order of preference.

One of the easiest measurables of a galaxy is its total luminosity. For 25 of the Calán/Tololo SN host galaxies we use our own CCD images (obtained with the CTIO Blanco 4-m or the 0.9-m telescope) to calculate instrumental magnitudes through concentric circular apertures (after removing foreground stars from the aperture). We perform the transformation of these magnitudes to the standard BV system using the photometric sequences around these galaxies (Hamuy et al. 1996c), and the corresponding color terms for the CTIO CCD cameras. For each galaxy we estimate its total magnitude from the curve of growth obtained. Since most of these galaxies lie well inside the Hubble flow we apply then K corrections that we compute from our own spectra of these galaxies. The next step is to correct these magnitudes for foreground reddening, which we perform using the values from Schlegel et al. (1998). Since there is no universally accepted method to correct the galaxy luminosities for internal absorption, we skip this correction. For 19 galaxies of the sample integrated magnitudes are readily available from the Third Reference Catalogue of Bright Galaxies (de Vaucouleurs et al. 1991, hereafter RC3). For consistency with our measurements we choose from RC3 the integrated mag-

nitudes B_T and V_T , which are uncorrected for internal absorption. Table 1 (columns 5-6) lists the integrated B_T and V_T magnitudes for such galaxies and the Calán/Tololo SN hosts. Also given in columns 7 and 8 are the absolute B and V magnitudes of the host galaxies, which we compute as follows. For the hosts of the nearby ($cz \leq 1000$ km sec⁻¹) SNe 1937C, 1972E, 1981B, 1989B, 1990N, and 1998bu we employ the Cepheid distances measured by Gibson et al. (2000). For the early-type hosts of the nearby SNe 1980N, 1986G, 1991bg, 1992A, and 1994D we use the SBF/PNLF distances listed in Hamuy et al. (1996a). For all of the other hosts with $cz \geq 2000$ km sec⁻¹ we use the recession velocity to compute the distance modulus, except for the host of SN 1996ai, whose redshift of 951 km sec⁻¹ is low enough to be affected by peculiar motion. To match the Cepheid distance scale of Gibson et al. (2000) we adopt $H_0=69$ km sec⁻¹ Mpc⁻¹.

3. Results

In this section we use the observations of the SN Ia host galaxies to explore the effect of the stellar environment on the SNe. To characterize a SN we use the decline rate, $\Delta m_{15}(B)$, which is defined as the amount that the SN declines in B band magnitude during the first 15 days after maximum light. It is a measure of the post-maximum decline rate, with fast-declining SNe having large $\Delta m_{15}(B)$ values and narrower light curves. This parameter proves to be a convenient reddening-free and distance-free estimate of the SN peak brightness (Phillips et al. 1999), with the peak luminosity decreasing with increasing decline rate.

The bottom panel of Figure 1 shows the morphological-type vs. $\Delta m_{15}(B)$ diagram for the objects of our sample. This plot confirms the result found by Hamuy et al. (1996a), namely, that elliptical galaxies have hosted only fast-declining SNe and that spirals produce preferentially slow-declining SNe. The top panel of Figure 1 shows the $B - V$ color of the host galaxies vs. $\Delta m_{15}(B)$. The remarkable feature of this “L-shaped” plot is the lack of fast-declining SNe among blue galaxies [$(B - V) \leq 0.7$]. Galaxies with $(B - V) \geq 0.7$, on the other hand, have produced SNe with a wide range of decline rates, which is somewhat different than the result of Branch et al. (1996) that revealed a lack of slow-declining SNe among red hosts. In any case, both diagrams point to the same conclu-

¹In three cases we use Hubble Space Telescope images secured through the “Supernova Host Galaxies” Cycle 6 SNAP program GO-6362. For the rest of the sample we employ ground-based CCD frames.

²The NASA/IPAC Extragalactic Database (NED) is operated by the Jet Propulsion Laboratory, California Institute of Technology, under contract with the National Aeronautics and Space Administration.

sion, namely, that the distribution of decline rates in elliptical galaxies is markedly different than that in spirals, in the sense that younger environments produce preferentially the slowest-declining (luminous) SNe (and vice versa).

The top panel of Figure 2 shows the absolute V magnitude of the host galaxies vs. $\Delta m_{15}(B)$. This plot reveals a trend for late-type galaxies, in the sense that the slowest-declining (brightest) events have been hosted by the least luminous galaxies. It is well known that the integrated luminosities of spirals are correlated (with a large scatter) with the oxygen abundance (Henry & Worthy 1999), presumably due to the fact that more massive galaxies have retained more of the metals ejected by SNe. Although the scatter in Figure 2 is substantial, this plot suggests that metal-poor environments (least luminous galaxies) harbor the brightest SNe (“dim galaxy-bright SN”). However, as we show in the bottom panel of Figure 2, it is the case that the least luminous galaxies of our sample are also the bluest. It is possible then that the metallicity effect suggested by the galaxy luminosities is instead an age effect, as suggested by Figure 1. Conversely, it is plausible that the age effect inferred by the galaxy colors is just a reflection of a metallicity effect.

What is clear from the integrated colors and luminosities of the SN Ia host galaxies is that both age and/or metallicity affect the luminosities of the SNe. It is important to try to disentangle these effects and a promising route to break this degeneracy is to use spectroscopic data for the host galaxies and the stellar population synthesis models of Worthey (1994) for absorption line strengths, at least in single-burst systems. In the Worthey models a single line index depends both on age and abundance but the Mg_2 - $H\beta$ plane (or other combinations of indices) permits, in principle, the removal of the “age-metallicity” degeneracy. Figure 3 shows such models for a wide range of ages (1.5-17 Gyr) and abundances between $[Fe/H] = -2$ and $+0.5$.

To populate this diagram with SN host galaxies we used the line strengths for the five early-type galaxies (NGC 1380, NGC 2962, NGC 4374, NGC 4526, and NGC 5061) observed by Trager et al. (1998, hereafter T98) at Lick Observatory with the IDS spectrograph (with a small entrance aperture of $1''.4 \times 4''$). High-quality line strengths for the central $r = r_e/8$ aperture of NGC 4374 were also obtained by González (1993, hereafter G93) with the IDS (and reproduced

by Trager et al. 2000; hereafter T00). In the rest of this paper we employ the G93 values for NGC 4374 and the T98 indices for the other cases. Since early-type galaxies display line-strength gradients, it proves necessary to calculate aperture corrections to convert the indices of T98, obtained through the rectangular aperture of $1''.4 \times 4''$, to the equivalent of the circular $r = r_e/8$ aperture of G93. For this purpose we compute synthetic line strengths through the circular and the rectangular apertures, and the corresponding difference between them, which we add to the observed index. The synthetic index is simply the luminosity-weighted line strength inside the specified aperture, using a $r^{1/4}$ law and the index gradients and zero-points from Davies et al. (1993) for $H\beta$ and Mg_2 , and from Kobayashi & Arimoto (1999) for Mg_b , $Fe5270$, and $Fe5335$ (in actuality, since an aperture correction is the difference between two synthetic line strengths, the zero point of the index does not affect our results). In all cases these corrections prove to be $\sim 15\%$ or less, in the sense of increasing $H\beta$ and decreasing the other indices. Table 2 lists the resulting absorption strengths for the five galaxies, which are overplotted on the model grid of Figure 3.

The first thing to notice in this figure is that two points lie outside the parameter space. The departure of NGC 5061 from the model grid can be simply understood as due to a young galaxy with high metal abundance. NGC 2962 poses more problems since the weak $H\beta$ value implies an age significantly larger than the Hubble time. It is possible that the weak $H\beta$ value is due to contamination by $H\beta$ emission. Emission is present near the center of $\sim 50\%$ of early-type galaxies (Davies et al. 1993) and may substantially bias the $H\beta$ absorption strength, especially on observations made through small apertures. A statistical correction based on $[O III]$ emission has been proposed (T00), but these values are not available for these galaxies. This problem can be overcome in the future with further observations of these galaxies through bigger apertures, to minimize the contamination by emission. With this caveat about the available data, we proceed with the determination of ages and abundances for these galaxies.

In principle we can use the Worthey line strength models to determine ages and metallicities. However, it is a well-known fact that the abundances derived from the Mg and the Fe indices yield $[Mg/Fe]$ ratios which exceed the solar values by 0.2–0.3 dex (Worthey et al. 1992). To account for this effect in what follows

we employ an extension of the Worthey models that incorporates non-solar abundances (T00), in order to derive single-stellar-population (SPP) equivalent ages, metallicities, and enhancement ratios, $[E/Fe]$, from the $H\beta$, Mgb , and $\langle Fe \rangle$ line strengths. Table 3 summarizes these values for the five early-type galaxies of our sample. The SPP ages span a wide range between 24 and 1.4 Gyr, in agreement with the finding of T00 from the sample of elliptical galaxies observed by G93. We find that the SPP abundances for the five galaxies span the range from $[Z/H] = -0.23$ to $+0.56$ which, again, is in fair agreement with the conclusion by T00 that early-type galaxies cover the range $-0.1 \leq [Z/H] \leq +0.7$. The enhancement ratios we derive here are also matched well by the strongly peaked ratios around $\langle [E/Fe] \rangle = +0.20$ found by T00 from the G93 sample.

The top panel of Figure 4 shows t_9 vs. $\Delta m_{15}(B)$, where t_9 is the SPP age in Gyr. Clearly the large error bars (mainly caused by the uncertainties in $H\beta$) and the small number of objects in this plot prevent us from drawing strong conclusions. Evidently, to be able to confirm or rule out an age effect on SNe Ia from this diagram it will be necessary in the future to secure high signal-to-noise spectra of as many early-type SN host galaxies as possible. The bottom panel of Figure 4 shows with open circles the $[Z/H]$ values for the five SN Ia host galaxies vs. $\Delta m_{15}(B)$. Note that in this case the uncertainties in $[Z/H]$ (mainly determined by the strong Mg feature) are quite low (typically 0.1–0.2 dex) which permit us to say that there appears to be a mild trend of metallicity with $\Delta m_{15}(B)$. Again, the low number of objects renders it difficult to draw any strong conclusion.

To populate this plot with more points we used the SIMBAD Astronomical Database to search for bibliographical references about metallicity measurements of the SN Ia spiral hosts listed in Table 1. This search yielded abundances for only three galaxies, namely, NGC 3368, NGC 5005, and NGC 5253. For NGC 5253 we adopt the value of Kobulnicky et al. (1999), $\log(O/H) = -3.86 \pm 0.02$, from nebular analysis of the integrated spectrum of the galaxy because this value represents a global measurement. Note that this value is in close agreement with the measurements of Storchi-Bergmann et al. (1994) [$\log(O/H) = -3.6$] and Campbell et al. (1986) [from $\log(O/H) = -3.64$ to -3.83]. For NGC 3368 we adopt the value at the effective radius r_e (11.2 kpc) quoted by Oey & Kennicutt (1993), $\log(O/H) = -2.96 \pm 0.02$, from nebular

analysis of three HII regions; this value is in good agreement with the analysis of 25 HII regions by Dutil & Roy (1999) who found a central abundance of $\log(O/H) = -3.02$ and a shallow abundance gradient of -0.009 dex kpc^{-1} . Finally, for NGC 5005 we adopt the characteristic abundance $\log(O/H) = -2.86 \pm 0.02$ at r_e (7.6 kpc) determined by Oey & Kennicutt (1993). Adopting the solar abundance (by mass) ratio $\log(O/H)_\odot = -1.93 \pm 0.07$ (Grevesse et al. 1996) we obtain the $[O/H]$ abundances for the three spirals of our sample which we include in Table 3.

To allow a comparison between the $[O/H]$ values of the late-type galaxies and the $[Z/H]$ abundances of the early-types we simply assume $[Z/H] = [O/H]$ for the latter, since O dominates Z in the line strength models. With the inclusion of the three spirals (shown as filled dots in Figure 4) there appears to be somewhat more evidence for a metallicity-decline rate relation for SNe Ia. There are a few caveats to keep in mind when examining this diagram. First, there are only 8 points in this diagram; second, the metallicities derived for spirals from HII regions studies are snapshots of the present-day abundance of the ISM in these galaxies, and it is likely that the metallicities of the SNe progenitors were even lower (since they formed earlier); third, the technique of nebular analysis in late-type galaxies and the method of absorption line indices in early-type galaxies for abundance determinations have not been tested on the same objects; and, fourth, we use global abundances for the host galaxies and not the values at the SN positions.

4. Discussion

To recapitulate, the photometric data of the SN Ia host galaxies show clear evidence that there are environmental conditions that affect the optical properties of SNe Ia. It is difficult though to identify whether the age or the metallicity of the stellar populations is responsible for the SN diversity, because the bluest galaxies of our sample are also the least luminous. In an attempt to disentangle the effects of age and metallicity we estimate SPP parameters for the five early-type galaxies with line strengths available in the literature, and we collect metallicities from nebular analysis of the emission spectra of three late-type galaxies. The spectroscopic data show that the age of the stellar population is not correlated with $\Delta m_{15}(B)$ and that metal-poorer environments produce the most luminous SNe. Given the low number

of galaxies in these diagrams and the large uncertainties in the SPP ages we must take these results with caution. In any case, the spectroscopic studies of the SN host galaxies provide a promising route to unveil the cause of the SNe Ia diversity, and it is important to start securing spectrophotometry of all SN host galaxies, both for a nebular analysis of the integrated emission spectrum of late-type galaxies and for a study of the absorption lines of the integrated spectrum of early-type galaxies.

If age was the main parameter responsible for the range of optical properties of SNe Ia, the photometric data suggest that younger environments produce preferentially slow-declining (luminous) SNe, which agrees with the theoretical predictions of Höflich et al. (1998). We will need to wait for further spectroscopic data, however, before we can confirm or rule out the role of age as the main SN parameter.

Despite the difficulties in identifying the driving parameter in the SN optical properties, the observations show that SNe Ia can occur in environments with a wide range of metallicities. This observation poses serious problems to the “strong wind” models advocated by Umeda et al. (1999) which predict the absence of SNe Ia in metal-poor environments. According to these models galaxies with $[\text{Fe}/\text{H}] \leq -1.0$ do not have WDs capable of blowing sufficiently strong winds to allow the WD mass to grow to the Chandrasekhar mass. This is contradicted by SN 1972E that went off in a very metal-poor environment ($[\text{Z}/\text{H}] \sim -2$). These models are also challenged by SNe 1996bi and 1998bu that exploded in galaxies with $[\text{Fe}/\text{H}] \sim -1.0$.

Given the present state of affairs and the difficulty to quantify the weights of these parameters in the SN properties, it is interesting to mention other pieces of observational data that could help us understand the nature of SNe Ia. Since galaxies, in general, display age and metallicity gradients, the study of the radial distribution of SNe in the host galaxies proves to be a useful tool for this purpose. According to the study by Wang et al. (1997), SNe Ia at smaller galactocentric distances have larger fluctuations in brightness than those farther out. Riess et al. (1999) reached the same conclusion using peak magnitudes uncorrected for extinction in the host galaxies. They also found that, when the magnitudes are corrected for extinction, SNe with projected separations of less than 10 kpc are 0.3 mag brighter than those farther out. A difficulty in the interpretation of these results comes

about by the use of projected galactocentric distances, since SNe at large distances can appear projected near the center of their hosts. In view of this problem Ivanov et al. (2000) have recently re-examined the radial distribution of SNe using *deprojected* distances in spiral galaxies, assuming that SNe Ia come from a disk population. After normalizing the SN radial distances by the size of the host galaxies, this study shows no indication of systematic changes of the SN magnitudes with radial distance. Given the abundance gradients observed in spiral galaxies (Henry & Worthy 1999), this result suggests that the metallicity effects on SNe Ia are small.

Another tool that can be used to identify the role of age in the SN properties is provided by the study of SN rates. According to Cappellaro et al. (1997) spiral galaxies are 50% more prolific than ellipticals in the production of SNe Ia. This result supports the claim that the SN rate (per unit galaxy luminosity) is enhanced in spirals, due to a population of SNe with younger progenitors.

In summary, both the theoretical and the observational studies provide support to the fact that age and metallicity can modify the properties of SNe Ia. It is unclear yet which of the two is the primary parameter. Since the theoretical studies have enormous uncertainties inherent to the physics of flame propagation, it is likely that the observational approach will provide the clues more quickly.

Besides the origin of the SN Ia diversity it is interesting to ask whether the environmental properties can bias the determination of distances by application of the $M/\Delta m_{15}(B)$ relation. Since the $(B - V)$ color of the SN host galaxies proves to be the best indicator of the environmental effect on the SN properties, we use this parameter in Figure 5 to examine this issue. The top panel shows the absolute V peak magnitude of the SNe Ia versus $(B - V)$ which confirms the result of Figure 2, i.e., that bluer galaxies on average produce brighter events. The bottom panel of Figure 5 shows the residuals of the Hubble diagram $[\mu - 5 \log(cz) + \text{constant}]$ versus $(B - V)$ which reveals that, despite the fact that the SN peak luminosities vary substantially with galaxy color, the distances inferred from the $M/\Delta m_{15}(B)$ relation do not depend on the environmental conditions. The formal fit to the residuals yields a slope which is only 1σ different than zero. At high redshifts we would expect younger and more metal-poor stellar populations, and therefore bluer galaxies. If the slight trend shown in Figure

5 was real, it would imply that the distances to the high- z SNe would be underestimated after application of the $M/\Delta m_{15}(B)$ relation. A correction for this bias (if any) would act to increase the distance to the high- z SNe and, thus, to provide further support to the conclusion that the cosmological constant is different from zero.

5. Conclusions

1) We confirm the result of Hamuy et al. (1996a) that the distribution of decline rates changes considerably with the morphological type of the SN host galaxies. We provide further evidence here from a much larger SN sample and the use of the $(B - V)$ color of the hosts, which reveals that brighter SNe occur in bluer environments. This suggests that the progenitor age determines the optical properties of SNe Ia.

2) We find some evidence that bright SNe occur in less luminous galaxies. In view that the galaxy luminosities are correlated with galaxy abundances, this correlation suggests that the diversity of SNe Ia is due to metallicity variations among the SN progenitors, in the sense that metal-poor environments produce the most luminous SNe.

3) At the moment it is difficult to separate the effects of ages and metallicities, because the galaxies of our sample show a correlation between color and luminosity.

4) A promising route to disentangle age and metallicity effects is to use spectroscopic data of the SN host galaxies. In our case the five galaxies with SPP abundances and ages, and the three galaxies with nebular analysis abundances seem to favor a metallicity effect, although the low number of objects and the large uncertainties prevent us from drawing strong conclusions.

5) We use the $(B - V)$ color of the SN host galaxies to quantify environmental effects in the determination of extragalactic distances using the $M/\Delta m_{15}(B)$ relation. Despite the fact that the SN peak luminosities vary substantially with galaxy color, the distances inferred from the $M/\Delta m_{15}(B)$ relation do not depend on the environmental conditions. This results lends credibility to the claim that the Universe is presently accelerating, due to a non-zero cosmological constant.

We are very grateful to Guy Worthey, D. Arnett, and D. Zaritsky for useful comments throughout the

preparation of this paper. Support for SCT was provided by NASA through Hubble Fellowship grant HF-01125.01-99A awarded by the Space Telescope Science Institute, which is operated by the Association of Universities for Research in Astronomy, Inc., for NASA under contract NAS 5-26555. PAP acknowledges support from the National Science Foundation through CAREER grant AST9501634, from the National Aeronautics and Space Administration through grant NAG 5-2798, and from the Research Corporation through a Cottrell Scholarship. This research has made use of the NASA/IPAC Extragalactic Database (NED) which is operated by the Jet Propulsion Laboratory, California Institute of Technology, under contract with the National Aeronautics and Space Administration.

REFERENCES

- Branch, D., Romanishin, W., & Baron, E. 1996, *ApJ*, 465, 73
- Campbell, A., Terlevich, R., & Melnick, J. 1986, *MNRAS*, 223, 811
- Cappellaro, E., Turatto, M., Tsvetkov, D.Y., Bartunov, O.S., Pollas, C., Evans, R., & Hamuy, M. 1997, *A&A*, 322, 431
- Davies, R.L., Sadler, E.M., & Peletier, R.F. 1993, *MNRAS*, 262, 650
- de Vaucouleurs, G., de Vaucouleurs, A., Corwin, H.G., Buta, R.J., Paturel, G., & Fouqué, P. 1991, *Third Reference Catalogue of Bright Galaxies* (Springer, Berlin) (RC3)
- Dutil, Y., & Roy, J. 1999, *ApJ*, 516, 62
- Gibson, B.K. et al. 2000, *ApJ*, 529, 723
- González, J. J., Ph.D. thesis, University of California, Santa Cruz (G93)
- Grevesse, N., Noels, A., & Sauval, A. J. 1996, in *Cosmic Abundances*, eds. S. S. Holt & G. Sonneborn, A.S.P. Conf. Ser., vol. 99 (San Francisco:ASP), P. 117
- Hamuy, M., Phillips, M. M., Maza, J., Suntzeff, N.B., Schommer, R.A., & Avilés, R. 1995, *AJ*, 109, 1
- Hamuy, M., Phillips, M. M., Suntzeff, N.B., Schommer, R.A., Maza, J., & Avilés, R. 1996a, *AJ*, 112, 2391

- Hamuy, M., Phillips, M. M., Suntzeff, N.B., Schommer, R.A., Maza, J., & Avilés, R. 1996b, AJ, 112, 2398
- Hamuy, M. et al. 1996c, 112, 2408
- Henry, R.B.C., & Worthey, G. 1999, PASP, 111, 919
- Höflich, P., Wheeler, J.C., & Thielemann, F.K. 1998, ApJ, 495, 617
- Ivanov, V. et al. 2000, in preparation
- Kobayashi, C. & Arimoto, N. 1999, ApJ, 527, 573
- Kobulnicky, H. A., Kennicutt, R. C., & Pizagno, J.L. 1999, ApJ, 514, 544
- Oey, M.S., & Kennicutt, R.C. 1993, ApJ, 411, 1370
- Perlmutter, S. et al. 1999, ApJ, 517, 565
- Phillips, M. M. 1993, ApJ, 413, L105
- Phillips, M. M., Lira, P., Suntzeff, N. B., Schommer, R. A., Hamuy, M., & Maza, J. 1999, AJ, 118, 1766
- Riess, A. G. et al. 1996, ApJ, 473, 88
- Riess, A. G. et al. 1998, AJ, 116, 1009
- Riess, A. G. et al. 1999, AJ, 117, 707
- Schlegel, D.J., Finkbeiner, D. P., & Davis, M. 1998, ApJ, 500, 525
- Storchi-Bergmann, T., Calzetti, D., & Kinney, A. L. 1994, ApJ, 429, 572
- Trager, S.C., Worthey, G., Faber, S. M., Burstein, D., & González, J. J. 1998, ApJS, 116, 1 (T98)
- Trager, S.C., Faber, S. M., Worthey, G., & González, J. J. 2000, astro-ph/0001072 (T00)
- Umeda, H., Nomoto, K., Kobayashi, C., Hachisu, I., & Kato, M., 1999, ApJ, 522, L43
- Wang, L., Höflich, P., & Wheeler, J.C. 1997, ApJ, 483, L29
- Worthey, G., Faber, S. M., & González, J. J. 1992, ApJ, 398, 69
- Worthey, G. 1994, ApJS, 95, 107

TABLE 1
PHOTOMETRIC OBSERVATIONS OF SN IA HOST GALAXIES

SN	$\Delta m_{15}(B)$ SN	Galaxy	Morph.	B_T GAL	V_T GAL	$M_B-5\log(H_0/69)$ GAL	$M_V-5\log(H_0/69)$ GAL	B-V GAL
1937C	0.87(10)	IC 4182	S/Irr	11.77(05)	11.38(12)	-16.65(09)	-17.02(14)	0.38
1972E	0.87(10)	NGC 5253	Irr	10.87(12)	10.44(12)	-16.96(16)	-17.34(16)	0.37
1980N	1.28(04)	NGC 1316	Sa pec	9.42(08)	8.53(08)	-21.89(10)	-22.76(10)	0.87
1981B	1.10(07)	NGC 4536	Sbc	11.16(08)	10.55(08)	-19.86(11)	-20.45(11)	0.59
1986G	1.73(07)	NGC 5128	S0+Spec	7.84(06)	6.84(08)	-20.48(09)	-21.37(10)	0.89
1989B	1.31(07)	NGC 3627	Sb	9.65(13)	8.92(13)	-20.54(21)	-21.24(21)	0.70
1990N	1.07(05)	NGC 4639	Sbc	12.24(10)	11.54(10)	-19.66(14)	-20.34(13)	0.67
1990O	0.96(10)	PGC 59955	SBa
1990T	1.15(10)	PGC 63925	Sa	15.61(10)	14.75(10)	-20.91(15)	-21.66(15)	0.75
1990Y	1.13(10)	anonymous	E?	16.86(10)	16.25(10)	-19.37(15)	-19.92(15)	0.55
1990af	1.56(05)	anonymous	SB0	16.56(10)	15.45(10)	-20.52(13)	-21.44(13)	0.92
1991S	1.04(10)	UGC 5691	Sb	15.67(10)	14.68(10)	-21.56(13)	-22.39(13)	0.83
1991T	0.94(05)	NGC 4527	Sbc	11.38(08)	10.52(09)	0.84
1991U	1.06(10)	IC 4232	Sbc	14.73(10)	13.91(10)	-21.36(17)	-22.09(17)	0.73
1991ag	0.87(10)	IC 4919	SBb	14.98(10)	14.34(10)	-19.17(33)	-19.73(33)	0.56
1991bg	1.93(10)	NGC 4374	E1	10.09(05)	9.11(05)	-21.33(07)	-22.27(07)	0.94
1992A	1.47(05)	NGC 1380	SA0	10.87(10)	9.93(10)	-20.20(14)	-21.12(14)	0.92
1992J	1.56(10)	anonymous	E/S0	15.67(10)	14.52(10)	-21.28(14)	-22.22(14)	0.94
1992K	1.93(10)	ESO 269-57	SBb	12.68(10)	11.81(10)	-21.19(41)	-21.93(41)	0.74
1992P	0.87(10)	IC 3690	SBa	15.55(10)	14.71(10)	-19.90(19)	-20.68(19)	0.78
1992ae	1.28(10)	anonymous	Scd/Sd	18.08(10)	17.43(10)	-19.78(12)	-20.27(12)	0.49
1992ag	1.19(10)	ESO 508-67	S
1992al	1.11(05)	ESO 234-69	Sb
1992aq	1.46(10)	anonymous	Sa?	19.09(10)	17.86(10)	-19.64(11)	-20.55(11)	0.91
1992au	1.49(10)	anonymous	E1
1992bc	0.87(05)	ESO 300-9	Sab	15.74(10)	15.02(10)	-19.09(24)	-19.75(24)	0.66
1992bg	1.15(10)	anonymous	Sa	16.15(10)	15.25(10)	-20.65(17)	-21.31(17)	0.65
1992bh	1.05(10)	anonymous	Sbc	16.57(10)	16.13(10)	-20.10(14)	-20.44(14)	0.34
1992bk	1.57(10)	ESO 156-8	E1	14.75(10)	13.82(10)	-22.61(13)	-23.33(13)	0.72
1992bl	1.51(10)	ESO 291-11	SB0/SBa	15.52(10)	14.51(10)	-21.06(14)	-21.95(14)	0.88
1992bo	1.69(05)	ESO 352-57	E5/S0	14.91(10)	13.95(10)	-19.78(26)	-20.65(26)	0.87
1992bp	1.32(10)	anonymous	S0/Sa	17.53(10)	16.56(10)	-20.70(12)	-21.40(12)	0.70
1992br	1.69(10)	anonymous	E0/1	18.51(10)	17.22(10)	-19.96(11)	-20.91(11)	0.95
1992bs	1.13(10)	anonymous	SBb	16.24(10)	15.61(10)	-21.14(12)	-21.65(12)	0.51
1993B	1.04(10)	anonymous	SBb	17.52(10)	16.80(10)	-20.37(12)	-20.91(12)	0.55
1993H	1.69(10)	ESO 445-66	SBb(rs)	14.72(10)	13.82(10)	-20.79(20)	-21.56(20)	0.78
1993O	1.22(05)	anonymous	E5/S01?	17.62(10)	16.74(10)	-19.50(13)	-20.22(13)	0.72
1993ac	1.19(10)	PGC 17787	E
1993ae	1.43(10)	IC 126	E
1993ag	1.32(10)	anonymous	E3/S01	16.68(10)	15.60(10)	-20.65(14)	-21.49(14)	0.83
1993ah	1.30(10)	ESO 471-27	SBb	15.56(10)	14.66(10)	-20.13(18)	-20.94(18)	0.81
1994D	1.32(05)	NGC 4526	S0	10.66(06)	9.70(06)	-20.29(10)	-21.23(10)	0.94
1994M	1.44(10)	NGC 4493	E
1994Q	1.03(10)	PGC 59076	S0
1994S	1.10(10)	NGC 4495	Sab

TABLE 1—*Continued*

SN	$\Delta m_{15}(B)$ SN	Galaxy	Morph.	B_T GAL	V_T GAL	$M_B-5\log(H_0/69)$ GAL	$M_V-5\log(H_0/69)$ GAL	B-V GAL
1994T	1.39(10)	PGC 46640	Sa
1994ae	0.86(05)	NGC 3370	Sc
1995D	0.99(05)	NGC 2962	S0	12.96(13)	11.93(13)	-19.88(58)	-20.85(58)	0.97
1995E	1.06(05)	NGC 2441	Sb	13.00(20)	12.19(21)	-20.63(42)	-21.41(43)	0.78
1995ac	0.91(05)	anonymous	S
1995ak	1.26(10)	IC 1844	Sbc
1995al	0.83(05)	NGC 3021	Sbc
1995bd	0.84(05)	UGC 3151	S
1996C	0.97(10)	MCG +08-25-47	Sa
1996X	1.25(05)	NGC 5061	E0	11.28(13)	10.36(13)	-21.64(57)	-22.49(57)	0.85
1996Z	1.22(10)	NGC 2935	Sb	12.10(14)	11.33(14)	-21.03(52)	-21.74(52)	0.71
1996ai	0.99(10)	NGC 5005	SBbc	10.61(08)	9.81(08)	0.79
1996bk	1.75(10)	NGC 5308	S0	12.31(15)	11.39(15)	-20.22(63)	-21.12(63)	0.90
1996bl	1.17(10)	anonymous	SBc
1996bo	1.25(05)	NGC 673	Sc	13.20(13)	12.61(13)	-21.36(30)	-21.88(30)	0.51
1996bv	0.93(10)	UGC 3432	S
1998bu	1.01(05)	NGC 3368	Sab	10.11(13)	9.25(13)	-20.19(16)	-21.03(16)	0.83

TABLE 2
LINE STRENGTHS OF SN HOST GALAXIES THROUGH $r_e/8$ APERTURE

SN	Galaxy	H β (Å)	Mg ₂ (mag)	Mgb (Å)	Fe5270 (Å)	Fe5335 (Å)	<Fe> (Å)
1991bg	NGC 4374	1.51(04)	0.243(016)	4.78(03)	2.94(04)	2.69(04)	2.82(03)
1992A	NGC 1380	2.08(24)	0.226(023)	4.15(45)	2.85(36)	2.39(42)	2.62(56)
1994D	NGC 4526	1.62(23)	0.248(024)	4.33(47)	3.00(36)	2.96(44)	2.98(57)
1995D	NGC 2962	1.23(26)	0.263(022)	3.92(44)	3.00(36)	2.62(42)	2.81(55)
1996X	NGC 5061	2.78(17)	0.238(015)	3.50(30)	2.74(24)	2.59(30)	2.67(39)

TABLE 3
AGES AND METALLICITIES OF THE SN IA HOST GALAXIES

SN	Age (Gyr)	[Z/H]	[E/Fe]	[O/H]
1972E	-1.93(07) ^a
1991bg	12.7(1.9)	+0.12(03)	+0.20(01)	...
1992A	3.3(4.3)	+0.26(20)	+0.23(12)	...
1994D	9.4(8.5)	+0.16(16)	+0.09(11)	...
1995D	24.3(7.2)	-0.23(12)	+0.01(10)	...
1996X	1.4(0.3)	+0.56(18)	+0.20(11)	...
1996ai	-0.93(07) ^b
1998bu	-1.03(07) ^b

^aKobulnicky et al. (1999)

^bOey & Kennicutt (1993)

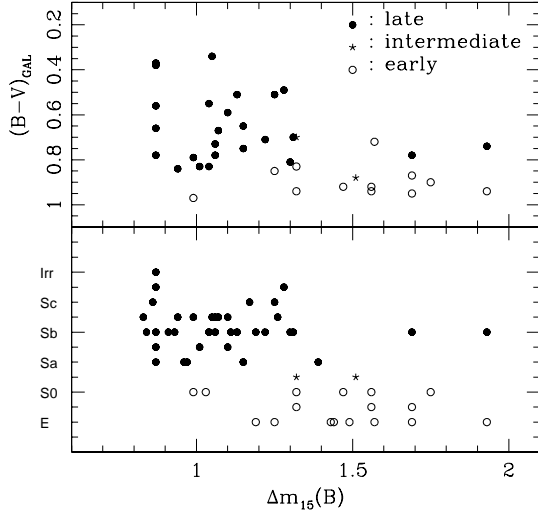


Fig. 1.— (top) The $(B - V)$ color of the SN host galaxy vs. the decline rate of the SN. (bottom) The morphological type of the SN host galaxy vs. the decline rate of the SN.

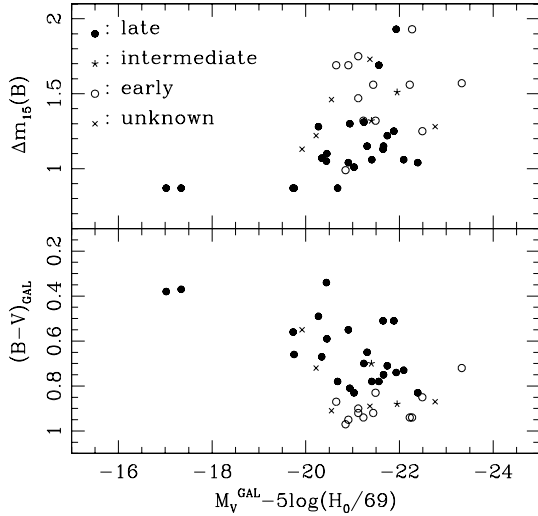


Fig. 2.— (top) The decline rate of the SN vs. the absolute V magnitude of the SN host galaxy. (bottom) The $(B - V)$ color vs. the absolute V magnitude of the SN host galaxy.

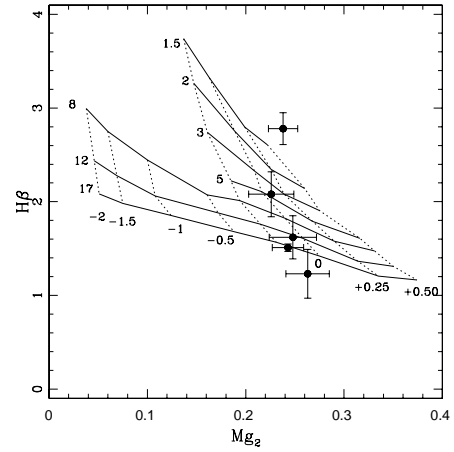


Fig. 3.— $H\beta$ versus Mg_2 relations as a function of age (1.5-17 Gyr) and metallicity ($-2 \leq [Fe/H] \leq +0.5$) from the population synthesis models of Worthey (1994). The galaxies listed in Table 2 are shown with solid dots.

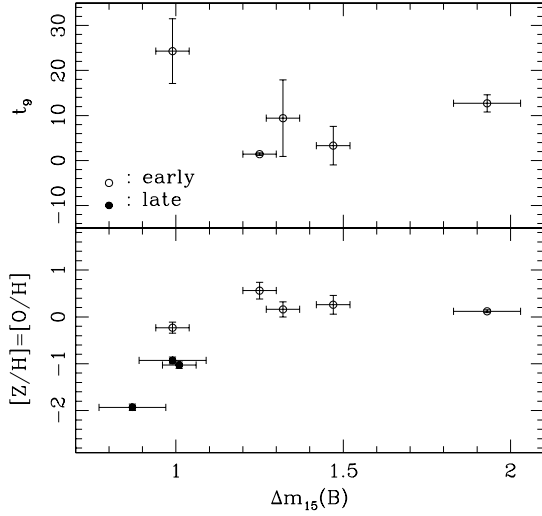


Fig. 4.— (top) The age (in units of Gyr) of the stellar populations of the SN host galaxies versus the decline rate of the SN. (bottom) Metallicity of the stellar populations of the SN host galaxies versus the decline rate of the SN.

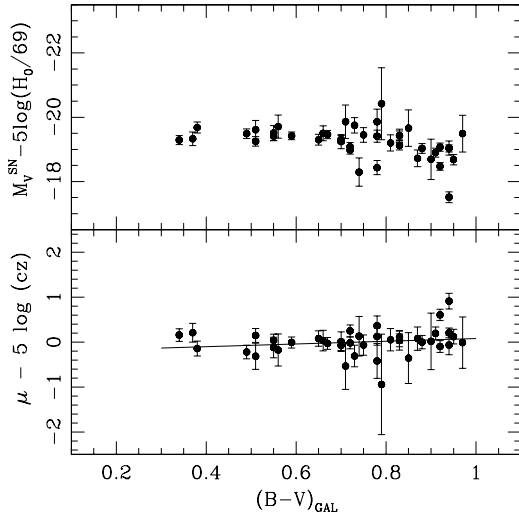


Fig. 5.— (top) The absolute V magnitude of the SN vs. the $(B - V)$ color of the SN host galaxy. (bottom) Residuals of the Hubble diagram in the V band vs. the $(B - V)$ color of the SN host galaxy.